



Uncertainty Propagation in Layered Unsaturated Soils

DARRIN D. DILLAH¹ and ANGELOS L. PROTOPAPAS^{2,*}

¹*SCS Engineers, Reston, Va., U.S.A.*

²*Department of Civil and Environmental Engineering, Polytechnic University, Brooklyn, New York, NY, U.S.A.*

(Received: 5 June 1998; in final form: 28 May 1999)

Abstract. This study analyzes the wetting front migration in layered unsaturated soils which have uncertain hydraulic properties. A Monte Carlo scheme was used to propagate the uncertainty of hydraulic parameters. RANUF, a computer program, was developed to solve the one-dimensional, pressure-based form of Richards' equation and to implement the Monte Carlo scheme.

Uncertainty propagation was investigated for two-layered soils of various alternating fine over coarse or coarse over fine layer configurations and of various nonrandomized and/or randomized layer arrangements. The effects of changing initial and boundary conditions were also investigated. Randomness was introduced via the saturated hydraulic conductivity, K_s , which was assumed to be distributed lognormally with a coefficient of variation of about 10 percent.

It was found that in layered soils the mean profiles (i.e., water content and pressure head) remained essentially unchanged regardless of which layer (or layers) was (or were) randomized; however, the variance profiles were affected. Also, higher uniform initial water content tended to inhibit uncertainty, but higher supply rates did not show any characteristic trend for uncertainty behavior.

Key words: uncertainty propagation, randomness of hydraulic properties, unsaturated flow model, Monte Carlo, heterogeneous soils, stochastic process.

1. Introduction

Understanding the dynamics of fluids as they infiltrate unsaturated porous media is of interest to various disciplines, e.g., agriculture, vadose zone contaminant transport, nuclear waste isolation, and landfill hydrology. Methods to predict wetting front positions in unsaturated media with perfectly known (deterministic) hydraulic parameters have been proposed for many years (e.g. Richards, 1931; Klute, 1952; Philip, 1957). More recent studies, though, have begun to investigate how transient wetting fronts in a single soil layer are affected by randomness in media hydraulic properties (e.g. Dagan and Bresler, 1983; Bresler and Dagan, 1983; Protopapas and Bras, 1990).

This study analyzes wetting front migration in layered unsaturated soils that have uncertain hydraulic properties. Richards' equation is the model used here

* Corresponding author.

to predict flow in unsaturated soils. Because of the complexities of this model, however, it is difficult to perform a complete statistical characterization (i.e., to identify the probability distribution) of the model's output due to variability of the soil's hydraulic properties. Consequently, various techniques have been developed to predict principal statistical properties, i.e., mean and variance, of the model's output. One such technique, the Monte Carlo method, is used in this study. It should be noted that theoretically, the Monte Carlo method could generate a large number of output realizations to provide complete statistical characterization, but computationally, it is impractical.

2. Hydraulic Parameters

In unsaturated soil, both the moisture content, θ , and the hydraulic conductivity, K , are related to the pressure head, ψ . The θ - ψ and K - ψ curves are known as the soil characteristic curves. During alternating wetting and drying events, these θ - ψ and K - ψ curves exhibit hysteresis. (However, since the cases analyzed in this study include only wetting events, this characteristic is not considered.) Various deterministic models which have a small number of unknown parameters have been developed to estimate the characteristic curves of a soil. In this study, the model employed by Bresler *et al.* (1978) is used:

$$\begin{aligned} S_e = 1, \quad \psi \geq \psi_{ae}, \quad S_e = \left(\frac{\psi_{ae}}{\psi}\right)^\beta, \quad \psi < \psi_{ae}, \\ K = K_s, \quad \psi \geq \psi_{ae}, \quad K = K_s \left(\frac{\psi_{ae}}{\psi}\right)^\alpha, \quad \psi < \psi_{ae}, \end{aligned} \quad (1)$$

where α and β are empirical coefficients, $S_e = (\theta - \theta_r)/(\theta_s - \theta_r)$ is effective saturation, ψ_{ae} is air entry pressure head value, θ_r is residual volumetric water content, θ_s is saturated volumetric water content, and K_s is saturated hydraulic conductivity. Table I presents measured parameters for two distinctly different soil types found in the literature.

When the hydraulic parameters are known at every point in space, the application of the above soil model is straightforward. However, perfectly accurate characterization is unlikely in 'real' soils; therefore, a stochastic alternative is employed. In the stochastic alternative, hydraulic parameters of a model (e.g. K_s , α , and β in Equation (1)) are assumed to have statistical distributions.

Table I. Parameters for soil model

Soil type	K_s (cm/day)	θ_s (cm ³ /cm ³)	θ_r (cm ³ /cm ³)	α	β	ψ_{ae} (cm)
Panoche clay loam	22.6	0.43	0.05	2.59	0.36	-15
Bet Dagan coarse soil	319.9	0.37	0.01	2.59	0.36	-15

Source: Bresler and Dagan (1983).

Since the hydraulic parameters have only positive values, this study assumes that the hydraulic parameters have lognormal distributions. This assumption reflects the fact that field data for most of the parameters are limited. However, the saturated hydraulic conductivity, K_s , has received more attention, and other investigators have confirmed that it follows a lognormal distribution (e.g. Russo and Bouton, 1992).

3. Numerical Solution of Richards' Equation

Considering a one-dimensional vertical unsaturated flow domain, the equation of flow is given by the one-dimensional Richards' equation as

$$\frac{\partial \psi}{\partial t} = \frac{1}{C(\psi)} \frac{\partial}{\partial z} \left[K(\psi) \left(\frac{\partial \psi}{\partial z} + 1 \right) \right], \quad (2)$$

where $\psi(z, t) = h - z$ is pressure head, $h(z, t)$ is hydraulic head, z is vertical coordinate (positive upward), $C(\psi) = d\theta/d\psi$ is specific moisture capacity, t is time, $\theta(\psi)$ is volumetric water content, and $K(\psi)$ is hydraulic conductivity.

This equation assumes nondeforming soil and single-phase, incompressible, and isothermal flow. The solution of Equation (2) requires the specification of boundary and initial conditions, and the soil characteristic curves $K(\psi)$ and $\theta(\psi)$.

Equation (2) is a nonlinear partial differential equation, for which analytical solutions are limited to simple cases. Numerical methods are, therefore, used to obtain solutions. Numerous numerical schemes have been developed to approximate Richards' equation, Equation (2). Here, a finite difference scheme similar to that used in Protopapas and Bras (1986, 1988) is employed. The end result is a collection of equations which are expressed in matrix form as

$$\mathbf{A}_f(\psi_\kappa, \xi) \psi_{\kappa+1} = \mathbf{e}(\psi_\kappa, \xi), \quad (3)$$

where $\psi_{\kappa+1}$ is a column vector of pressure heads at N discrete nodes at time $\kappa + 1$, \mathbf{A}_f is a tridiagonal $N \times N$ matrix, \mathbf{e} is a $N \times 1$ vector function, and ξ is a vector with the parameters that control the functions $K(\psi)$ and $C(\psi)$ at each node in the soil profile. Since \mathbf{A}_f is a tridiagonal matrix, a direct, fast, and simple algorithm (i.e. Thomas algorithm) is used to solve Equation (3) for the pressure head, $\psi(z, t)$. The soil moisture profile, $\theta(z, t)$, is then computed from $\psi(z, t)$ and the soil characteristic curve, $\theta(\psi)$.

The numerical scheme was coded using FORTRAN 90. The resulting program is named RANUF. Some features of the program follow:

- Handles unlimited soil layers.
- Uses either Equation (1) or Van Genuchten (Van Genuchten, 1980) soil curves.
- Allows soil parameter specification for all nodes; any can be specified as random.

- Allows positive pressures within the profile; i.e. it solves saturated flow problems.
- Implements Monte Carlo simulations.

4. Monte Carlo Technique

In the Monte Carlo technique, one or more hydraulic parameters are randomized, but it is assumed that their probability distribution functions are known. Based on their probability distribution functions, M values of each hydraulic parameter are randomly selected. For each sample set, the $K(\psi)$ and $\theta(\psi)$ curves are computed (via Equation (1)), and the flow model (Equation (2)) is solved to generate M outcomes of ψ and θ profiles at any given time, κ . At time, κ , first and second moments (mean and variance) of the M outcomes are determined at each node in the profile. The number of simulations, M , is made large enough so that mean and variance of the ψ and θ profiles are insensitive to increasing values of M ; i.e. further increase in the number of simulations beyond M , produces essentially the same profiles.

The Monte Carlo technique for propagating uncertainty in unsaturated soils has been coded into RANUF. The program uses Equation (1), to model the soil characteristic curves. An input file is used to specify the hydraulic parameters at all nodes in the profile, and any parameter can be specified as being random. RANUF assumes that each randomized parameter fits a lognormal probability distribution function. In addition to the hydraulic parameters, other inputs are specified such as boundary conditions, initial conditions, time steps, spatial discretization, and number of simulations, M . After entering all the input data, RANUF automatically uses the Monte Carlo technique to determine mean and variance profiles of ψ and θ at any specified times.

It is important to note that RANUF is based on a numeric scheme that has been demonstrated to be free from numerical dispersion, when applied to soils with deterministic properties (Protopapas and Bras, 1986, 1988). Since the uncertainty results are statistics of a set of 'deterministic' results, it may be induced that the uncertainty results are also free from numerical dispersion.

5. Results and Analysis

In this section, uncertainty propagation results are presented and analyzed for various two-layer soil configurations, composed of both fine- and coarse-textured soils. The fine-textured soil used is the Panoche clay, and the coarse-textured soil is the Bet Dagan coarse soil. Both soils are parameterized by Equation (1), as presented in Table I.

Table II summarizes the various two-layered cases considered. All profiles consist of a 20 cm soil layer over a 60 cm layer. In each configuration, either the

Table II. Cases investigated for two-layered soils

Case no.	Random layer	Top layer	Bottom layer	Condition investigated	Figure no.*
1	Bottom	Fine	Coarse	Time	1, 3a, 6a
2	Bottom	Coarse	Fine	Time	2, 3b, 6b
3	Top	Fine	Coarse	Time	2, 4a, 7a
4	Top	Coarse	Fine	Time	2, 4b, 7b
5	Both	Fine	Coarse	Time	2, 5a, 8a
6	Both	Coarse	Fine	Time	2, 5b, 8b
7	Bottom	Fine	Coarse	Time & w.c.	9a, b
8	Bottom	Coarse	Fine	Time & Q_{top}	10a, b

*Refers to figure number where results are plotted.

fine soil overlies the coarse soil or the coarse overlies the fine. Each individual layer is homogeneous, but each has either a randomized or deterministic saturated hydraulic conductivity, K_s . All randomized K_s are assumed to fit a lognormal probability distribution function with a coefficient of variation equal to 10 percent; e.g. if the average K_s is 319.9 cm/day, the standard deviation will be 31.19 cm/day. For each case, 150 is used for M . (Increases in M , up to 1000 simulations, produced essentially the same results.) The behavior of the flow statistics is studied as the wetting front penetrates an initially-uniform moist layered soil, under a constant supply rate. The effects of changing either the uniform initial water content or supply rate are also studied.

The profile configurations, coefficient of variation, and boundary and initial conditions used in this study do not simulate any particular field situation, but they are selected so that the behavior of uncertainty could be investigated for various two-layered configurations (coarse over fine or fine over coarse), where at least one layer contains a small randomization.

Figures 1–10 present the results. Figures 1 and 2 show the progression of pressure head and water content in fine soil over coarse soil and coarse soil over fine soil, respectively. Figures 3–5 allow a comparison of variance growth for fine soil over coarse soil and coarse soil over fine soil that have various nonrandomized and/or randomized layer arrangements. Figures 6–8 show how pressure head and water content coefficients of variation grow in fine soil over coarse soil and coarse soil over fine soil that have various nonrandomized and/or randomized layer arrangements. Finally, Figures 9 and 10 show, for selected cases, how the results are affected with an increase of initial water content and supply rate, respectively. The specific initial and boundary conditions and specific simulation times are given in each figure. Appropriate time and space steps were employed in the simulations to obtain accurate results.

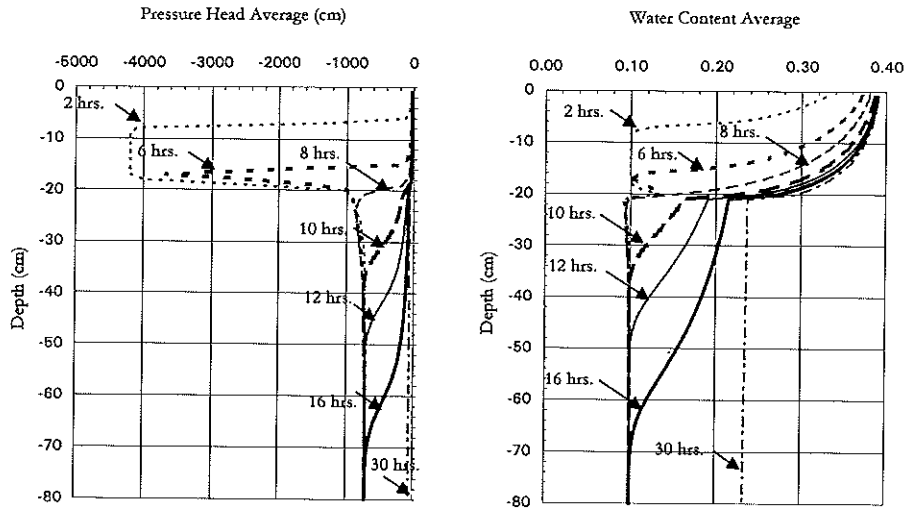


Figure 1. Pressure head and water content mean profiles for Panoche over Bet Dagan; supply rate = 12 cm/day; Init. w.c. = 0.1; profiles are similar regardless of which layer(s) is (are) randomized.

Analyses of the results for the two-layer soils follow:

A. Bottom layer randomized

Fine soil over randomized coarse soil. Figures 1, 3(a), and 6(a) show the results for specific times during the front propagation. Basic characteristics of these results follow:

- Immediately after infiltration begins, a variance of approximately 40^2 cm^2 is observed at the layer interface (hereinafter referred to as ‘interface variance’), (see Figure 3(a)). The interface variance is localized at the interface, and as time progresses and as the wetting front continues its approach and finally passes the interface, the interface variance steadily decreases and becomes negligible. The variance that appears in the upper nonrandomized layer is due to pressure equilibration that occurs when two contrasting soil layers with equal uniform initial moisture contents are placed together – Dillah (1998) describes this phenomenon in more detail.
- From beginning to end of the infiltration process, the variance within the upper nonrandomized layer remains essentially zero.
- As the wetting front enters the lower randomized layer, the variance exhibits a peak at the front (hereinafter referred to as ‘front peak’). This front peak then moves with the front and grows with time.
- After the wetting front passes through the bottom of the lower layer, the pressure head coefficient of variation (CV_ψ) and the water content coefficient of variation (CV_θ) both attain relatively constant steady-state values within the lower randomized layer (see Figure 6(a)).

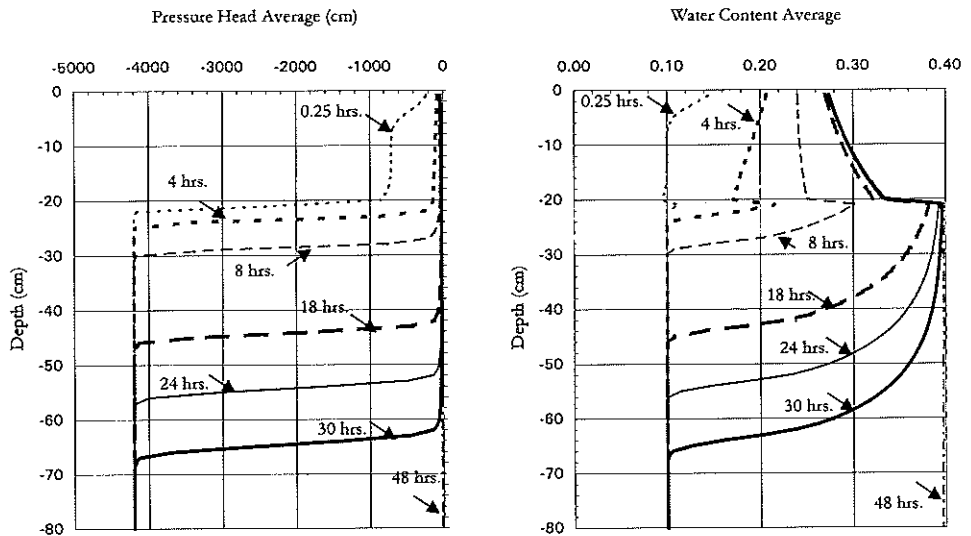


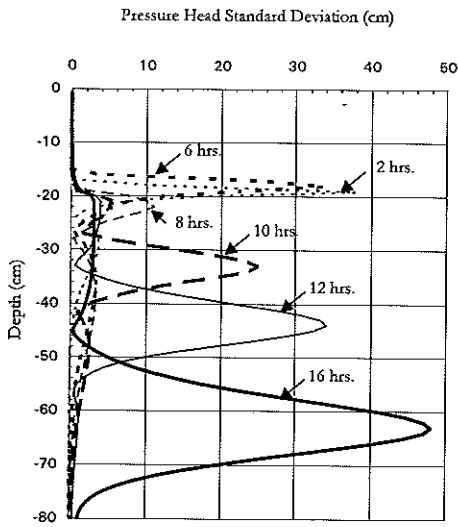
Figure 2. Pressure head and water content mean profiles for Bet Dagan over Panoche; supply rate = 12 cm/day; Init. w.c. = 0.1; profiles are similar regardless of which layer(s) is (are) randomized.

Figures 9(a) and 9(b) illustrate how the results are affected when the uniform initial water content θ_i is increased. The above listed basic characteristics are not affected. However, the following are observed:

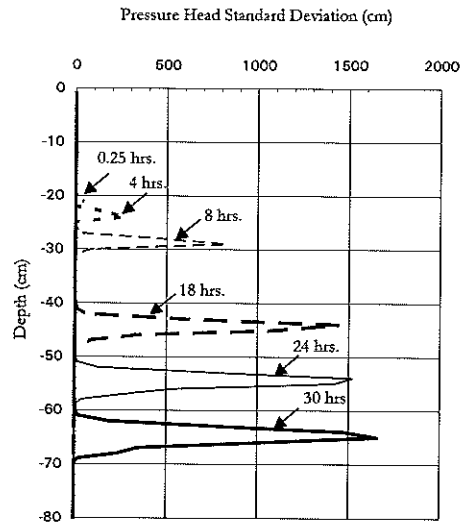
- Wetting fronts penetrate faster.
- Smaller interface variances are observed at equal early times, when variance is nonzero at the interface.
- In the randomized layer, smaller front peaks are observed at equal times.
- For equal times prior to steady state, values of CV_ψ and CV_θ at the layer interface are lesser for wetter soil (see Figure 9(b)). As steady state is approached, however, it is observed that θ_i has negligible effect on the steady-state mean profiles (of ψ and θ) and that the CV_ψ and CV_θ profiles are about equal.

Coarse soil over randomized fine soil. Figures 2, 3(b), and 6(b) show the results for specific times during the front propagation. The characteristics are similar to the basic characteristics given above for the fine soil over randomized coarse soil. However, in this case, the front variance in the lower randomized layer is significantly greater. That is, the front (peak) variance is larger in the lower randomized layer when the layer's texture is finer. It is also observed that the mean profiles have a sharper front in the finer layer, and the spread of the front variance is smaller.

Figures 10(a) and 10(b) show the results for a supply rate greater than the average saturated hydraulic conductivity, μ_{Ks2} , of the bottom fine layer, but less than the μ_{Ks1} of the top coarse layer. Under these conditions an inversion of the pressure head gradient occurs – refer to Dillah (1998) for a detailed discussion concerning

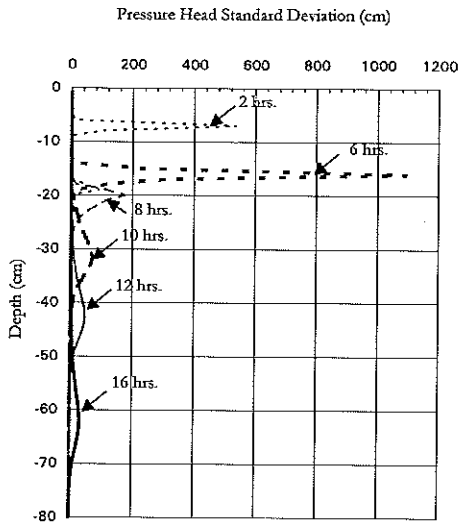


a. Panoche over random Bet Dagan

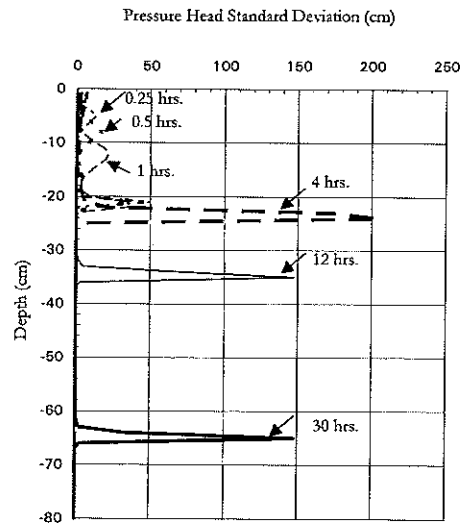


b. Bet Dagan over random Panoche

Figure 3. Variance growth in two-layered soils; bottom layer randomized; supply rate = 12 cm/day; Init. w.c. = 0.1.



a. Random Panoche over Bet Dagan



b. Random Bet Dagan over Panoche

Figure 4. Variance growth in two-layered soils; top layer randomized; supply rate = 12 cm/day; Init. w.c. = 0.1.

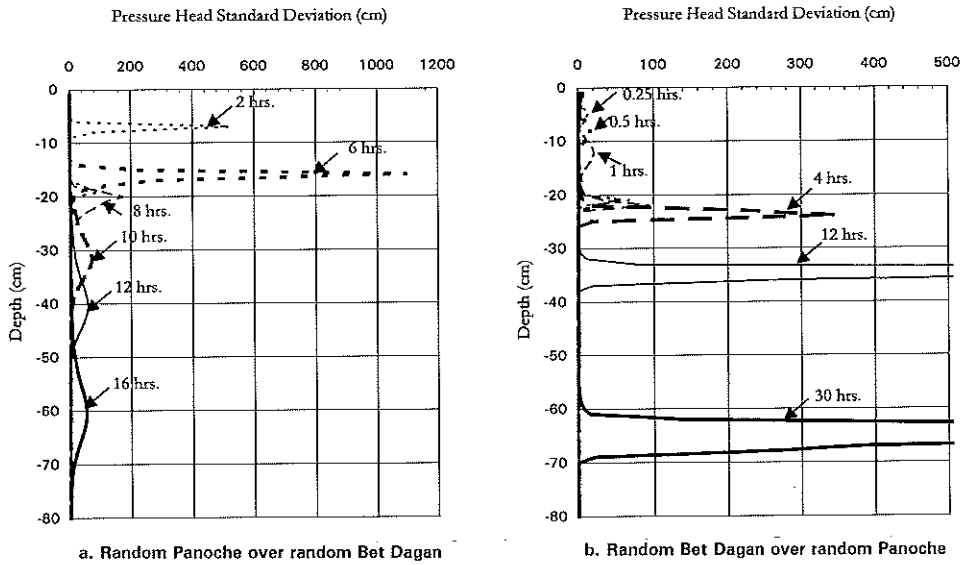


Figure 5. Variance growth in two-layered soils; both layers randomized; supply rate = 12 cm/day; Init. w.c. = 0.1.

the flow dynamics of pressure head gradient inversion. Comparing these results to the results found for a lower supply rate (i.e. comparing to Figures 2, 3(b), and 6(b)), it is observed that:

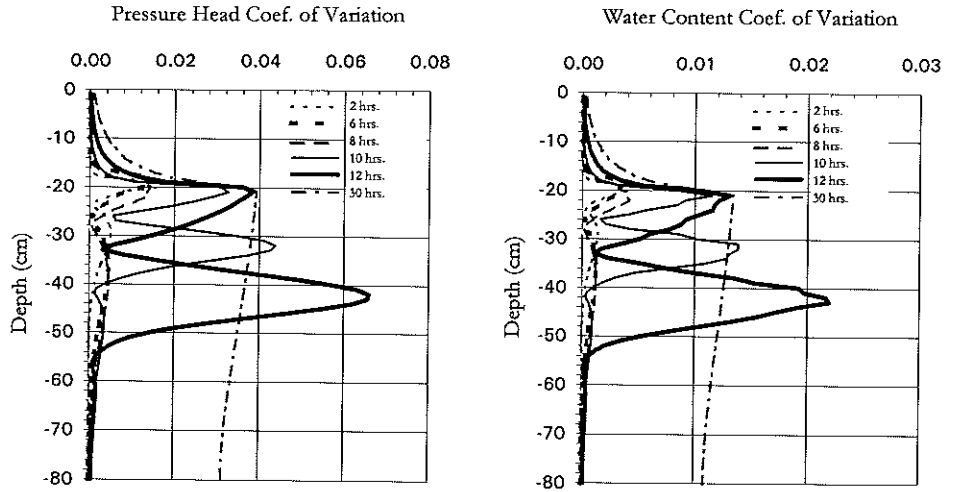
- The wetting front penetrates faster.
- The variance peak does not continuously grow with time – a dip is observed approximately midway within the lower layer.
- For higher supply rates, the CV_{θ} steady-state values decrease. Although the CV_{ψ} profile is not shown here, the CV_{ψ} steady-state values also decrease.

B. Top layer randomized

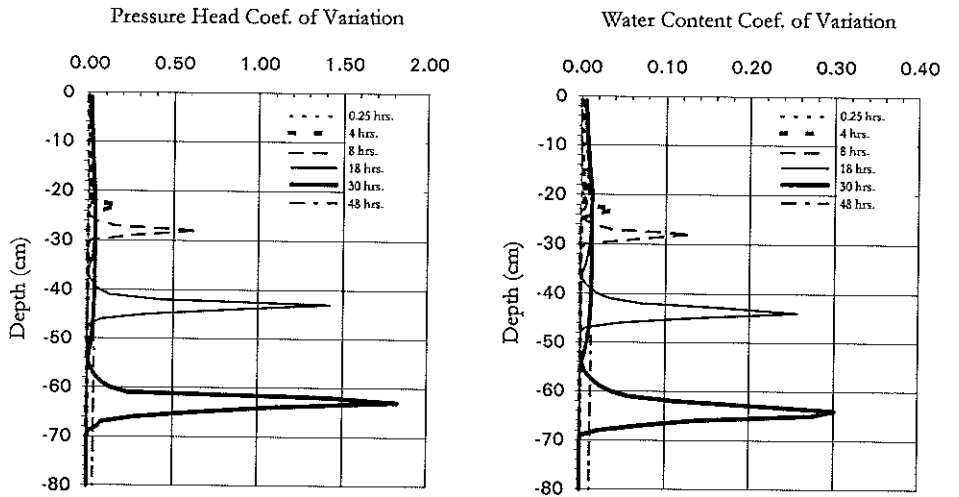
Randomized fine soil over coarse soil. The mean profiles obtained for this simulation were similar to the profiles obtained for fine over randomized coarse simulation (Figure 1); therefore, the profiles were not reproduced. Consequently, based on the simulations performed in this study, it has been found that similar mean profiles are obtained regardless of which layer is randomized.

Figures 4(a) and 7(a) show the other results for specific times during the front propagation. Basic characteristics of the results follow:

- Immediately after infiltration begins, an interface variance is observed that has similar magnitude as in the fine soil over randomized coarse soil case (see Figure 4(a)). As time progresses and as the wetting front approaches and passes the interface, the interface variance decreases and becomes negligible. The variance that appears in the upper nonrandomized layer is due to pressure equi-

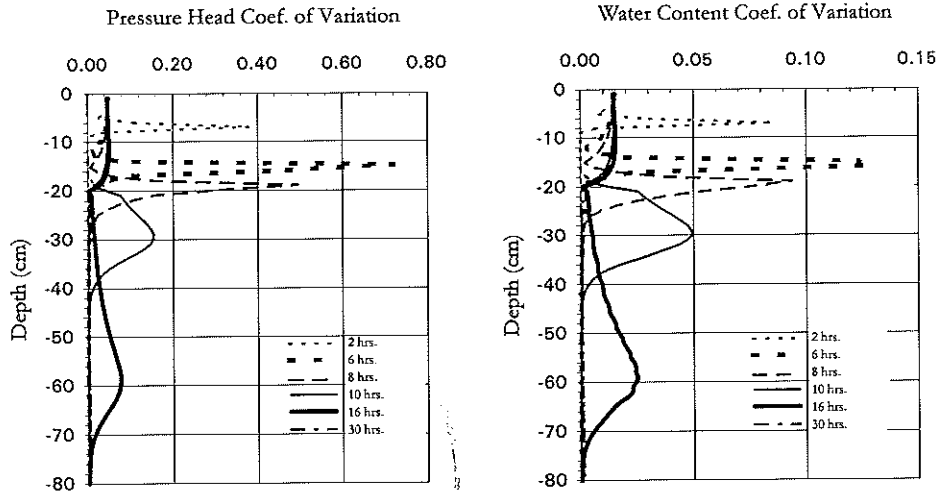


a. Panoche over random Bet Dagan

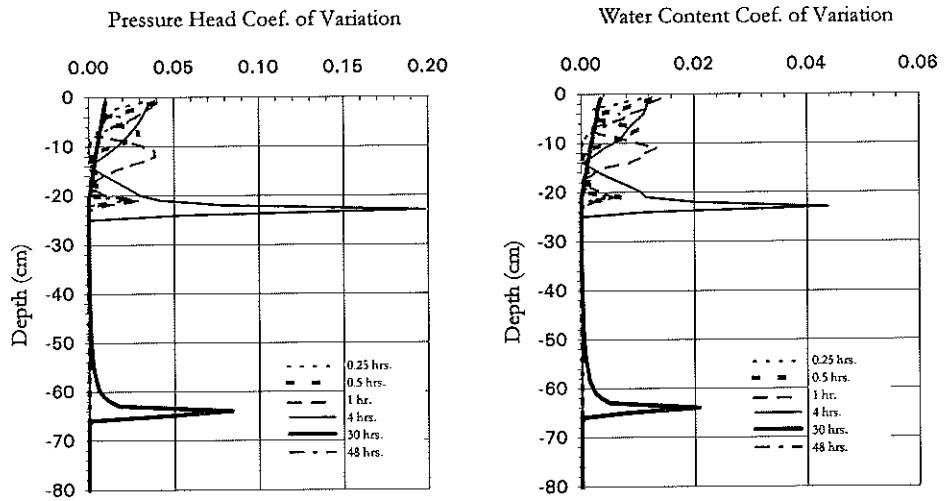


b. Bet Dagan over random Panoche

Figure 6. Coefficient of variation growth in two-layered soils; bottom layer randomized; supply rate = 12 cm/day; Init. w.c. = 0.1.

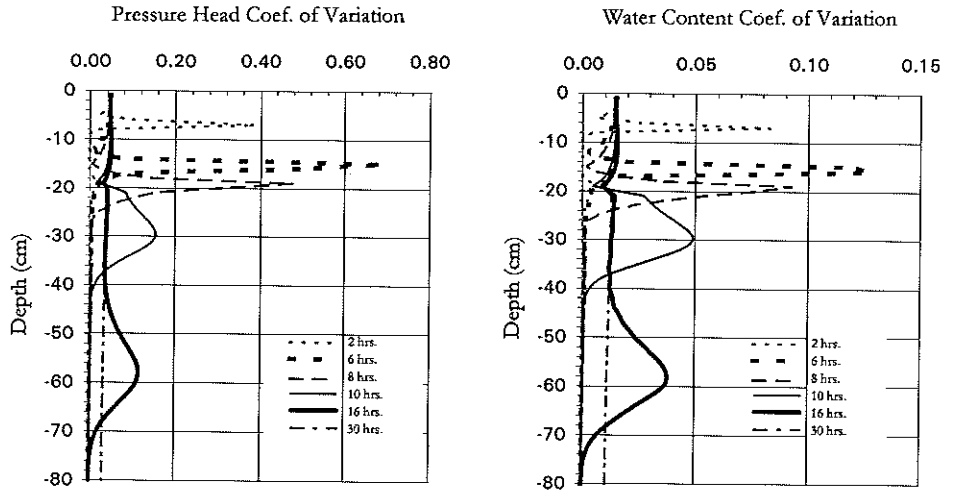


a. Random Panoche over Bet Dagan

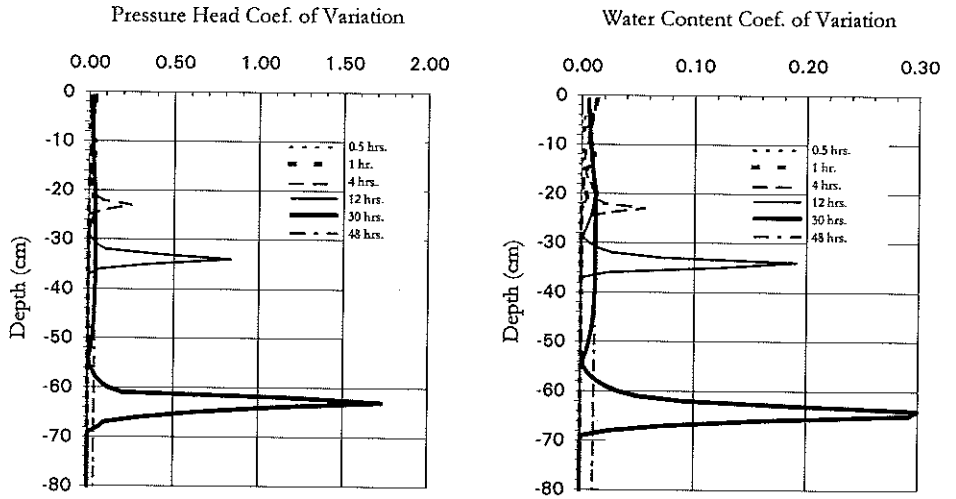


b. Random Bet Dagan over Panoche

Figure 7. Coefficient of variation growth in two-layered soils; top layer randomized; supply rate = 12 cm/day; Init. w.c. = 0.1.

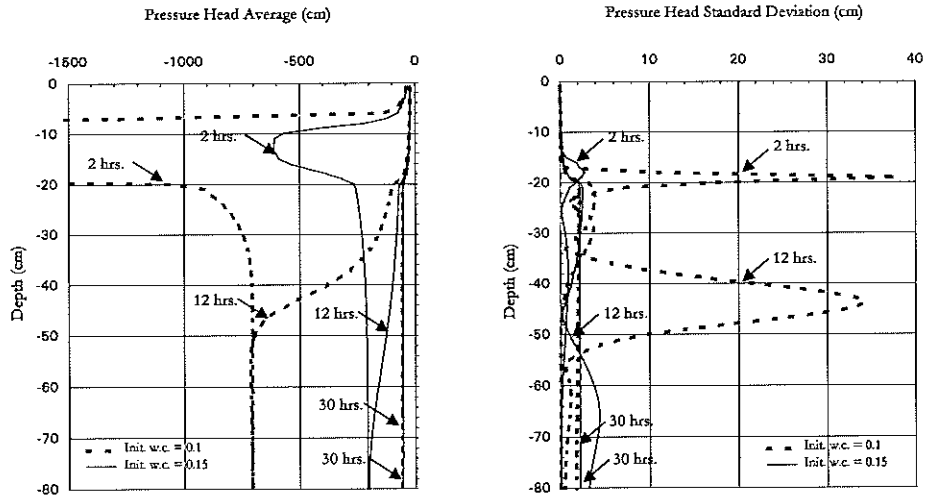


a. Random Panoche over Random Bet Dagan

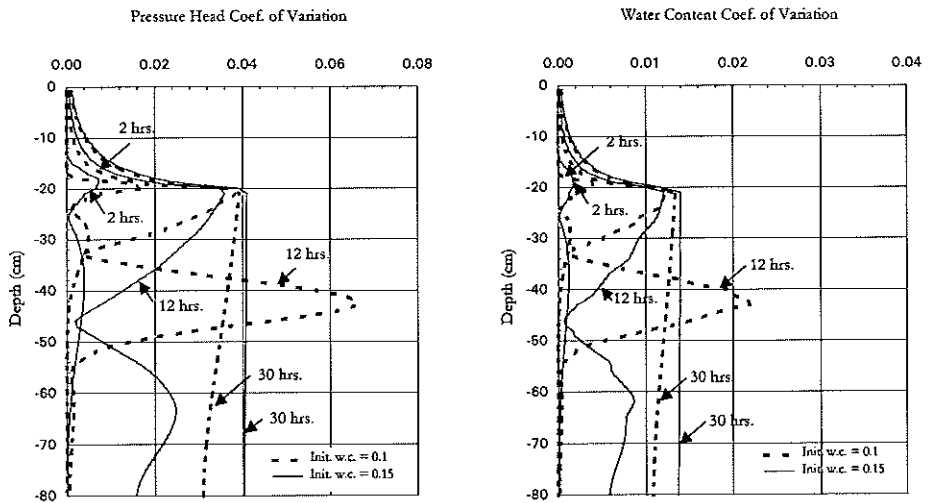


b. Random Bet Dagan over Random Panoche

Figure 8. Coefficient of variation growth in two-layered soils; both layers randomized; supply rate = 12 cm/day; Init. w.c. = 0.1.



a. Pressure head mean and standard deviation



b. Pressure head and water content coef. of variation

Figure 9. Investigation of how uniform initial water content affects results; Panoche over random Bet Dagan; supply rate = 12 cm/day.

libration that occurs when two contrasting soil layers with equal uniform initial moisture contents are placed together. As mentioned, Dillah (1998) describes this phenomenon in more detail.

- As the wetting front penetrates the upper randomized layer, the variance exhibits a peak at the front. This front peak moves with the front and grows with time, until it reaches the layer interface. The front variance is much larger than the interface variance.
- As the wetting front enters the lower nonrandomized layer, the variance continues to exhibit a peak at the front. However, this peak steadily decreases as the front passes through the lower layer (see Figure 4(a)). Also during this time phase, CV_{ψ} and CV_{θ} attain relatively constant steady-state values within the upper randomized layer (see Figure 7(a)).
- After the wetting front passes through the bottom of the lower layer, steady-state CV_{ψ} and CV_{θ} values remain within the upper randomized layer. However, CV_{ψ} and CV_{θ} values in the lower nonrandomized layer become negligible (see Figure 7(a)).

Randomized coarse soil over fine soil. The mean profiles obtained for this simulation were similar to the profiles obtained for coarse over randomized fine simulation (Figure 2); therefore, the profiles were not reproduced. This finding agrees with the previous finding that similar mean profiles are obtained regardless of which layer is randomized.

Figures 4(b) and 7(b) show the other results for specific times during the front propagation. The characteristics are similar to the basic characteristics given above

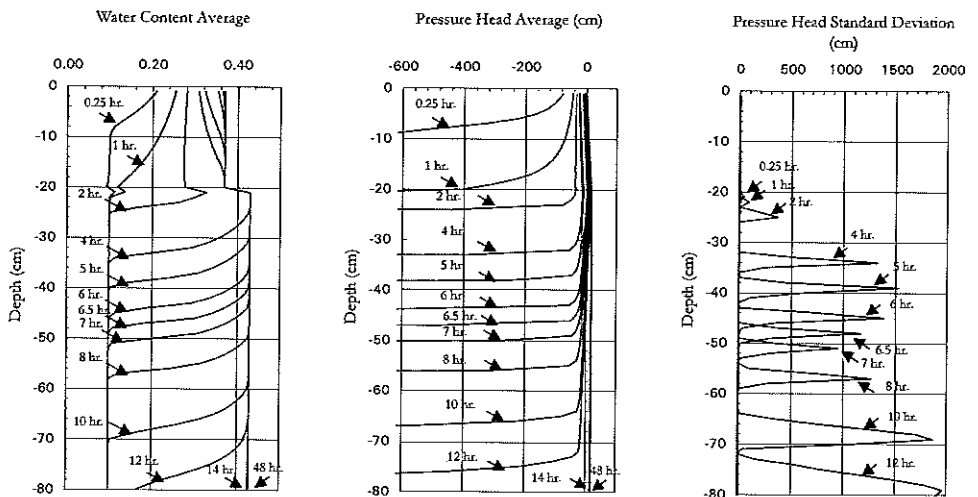


Figure 10a. Investigation of how supply rate affects results; Bet Dagan over random Panoche; supply rate = 50 cm/day; Init. w.c. = 0.1.

Water Content Coef. of Variation

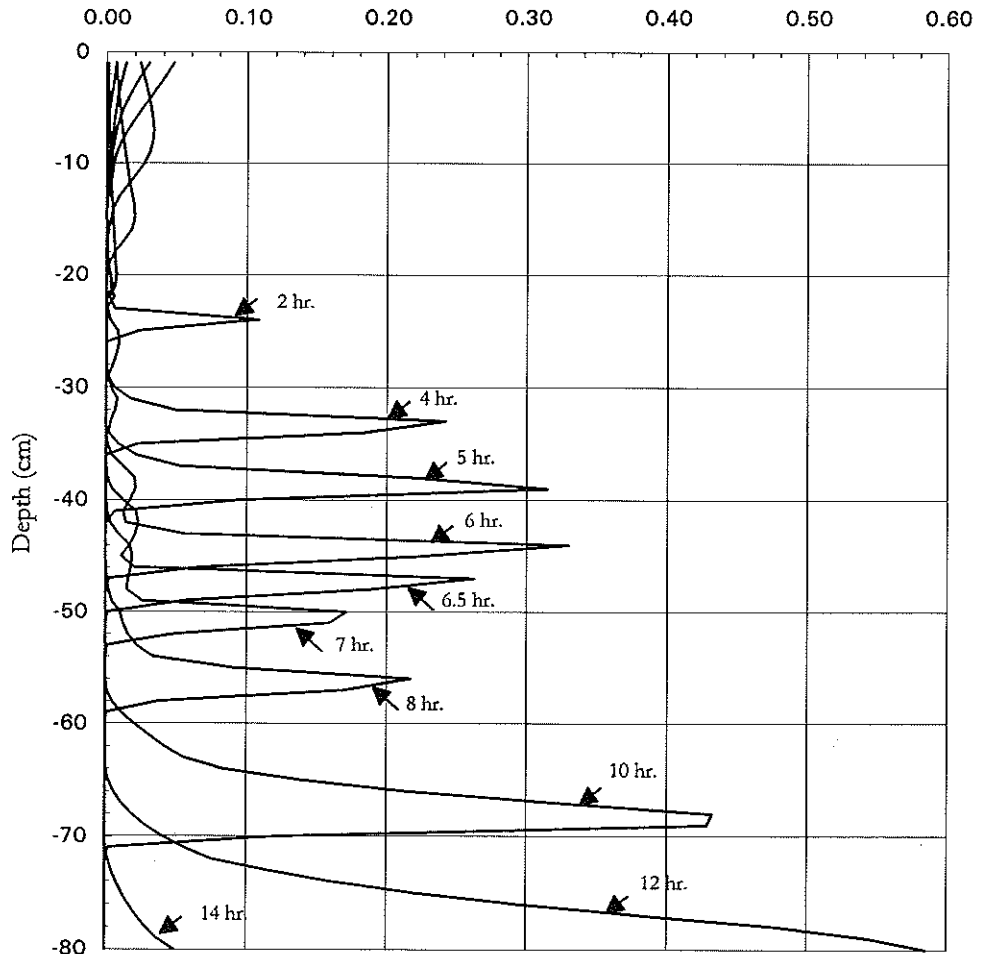


Figure 10b. (continued)

for the randomized fine soil over coarse soil. However, in this case, the front variance in the upper coarse-textured randomized layer is significantly lesser. Also, as the wetting front enters the lower, fine-textured, nonrandomized layer, the front variance initially increases (beyond the values in the upper layer); then, it decreases as the front penetrates through the layer.

C. Both layers randomized

Randomized fine soil over randomized coarse soil. The mean profiles obtained for this simulation were similar to the profiles obtained for the previous fine over

coarse simulations (Figure 1); therefore, the profiles were not reproduced. Again, this finding agrees with the previous finding that similar mean profiles are obtained regardless of which layer (or layers) is (or are) randomized.

Figure 5(a) and 8(a) show the other results for specific times during the front propagation. Basic characteristics of the results follow:

- Immediately after infiltration begins, an interface variance is observed that has similar magnitude as in previous cases, i.e. approximately 40^2 cm^2 . As time progresses and as the wetting front approaches and passes the interface, the variance at the interface decreases and becomes negligible.
- As the wetting front penetrates the upper layer, the variance exhibits a peak at the front. This front peak moves with the front and grows with time, until it reaches the layer interface. The front variance in the upper fine layer is much larger than the interface variance (see Figure 5(a)).
- As the wetting front enters the lower layer, the variance continues to exhibit a peak at the front. However, the front peak drops considerably from its value in the upper fine layer. As the front passes through the lower layer, the peak remains relatively constant (see Figure 5(a)). Also during this time phase, CV_ψ and CV_θ attain relatively constant steady-state values within the upper randomized layer (see Figure 8(a)).
- After the wetting front passes through the bottom of the lower layer, relatively constant steady-state CV_ψ and CV_θ values remain within the upper randomized layer (see Figure 8(a)). Within the lower randomized layer, CV_ψ and CV_θ also attain relatively constant steady-state values.

Randomized coarse soil over randomized fine soil. The mean profiles obtained for this simulation were similar to the profiles obtained for the previous coarse over fine simulations (Figure 2); therefore, the profiles were not reproduced. Again, this finding agrees with the previous finding that similar mean profiles are obtained regardless of which layer (or layers) is (or are) randomized.

Figures 5(b) and 8(b) show the other results for specific times during the front propagation. Basic characteristics of the results follow:

- Immediately after infiltration begins, an interface variance is observed that has similar magnitude as in previous cases, i.e. approximately 60^2 cm^2 (see Figure 5(b)). As time progresses and as the wetting front approaches and passes the interface, the variance at the interface decreases and becomes negligible.
- As the wetting front penetrates the upper layer, the variance exhibits a peak at the front. This front peak moves with the front and grows with time, until it reaches the layer interface.
- As the wetting front enters the lower layer, the variance continues to exhibit a peak at the front. However, the peak increases considerably from its value in

the upper coarse layer. As the front passes through the lower layer, the front peak again continues to grow.

- After the wetting front passes through the bottom of the lower layer, steady-state CV_ψ and CV_θ values remain within both upper and lower randomized layers (see Figure 8(b)).

6. Conclusions

The main conclusions of this study are summarized in the following:

1. In layered soils the mean profiles (i.e. water content and pressure head) remain essentially unchanged regardless of which layer (or layers) is (or are) randomized; however, the variance profiles are affected.
2. Increases in uniform initial water content cause the variance peaks to decrease; thus, higher uniform initial water content tends to reduce uncertainty in wetting front propagation.
3. Increases in supply rate do not show any characteristic trend for uncertainty behavior.

Note that the methodology used in this study is general, and it is not limited to the cases presented here. In fact, Dillah (1998) uses this methodology to generate uncertainty results for homogeneous and four-layered soils. Also, in addition to K_s randomization, he considers randomization of other hydraulic parameters (e.g. α and β), both individually and collectively.

References

- Bresler, E. and Dagan, G.: 1983, Unsaturated flow in spatially variable fields. 2. Application of water flow models to various fields, *Water Resour. Res.* **19**, 413–420.
- Bresler, E., Russo, D. and Miller, R. D.: 1978, Rapid estimate of unsaturated hydraulic conductivity function, *Soil Sci. Soc. Am. J.* **42**, 170–172.
- Dagan, G. and Bresler, E.: 1983, Unsaturated flow in spatially variable fields. 1. Derivation of models of infiltration and redistribution, *Water Resour. Res.* **19**, 413–420.
- Dillah, D. D.: 1998, Uncertainty propagation and wetting front instability in unsaturated porous media, PhD Diss., Department of Civil and Environmental Engng, Polytechnic Univ., Brooklyn, NY.
- Van Genuchten, M. Th.: 1980, A closed-form equation for predicting the hydraulic conductivity of unsaturated soils, *Soil Sci. Soc. Am. J.* **44**, 892–898.
- Klute, A.: 1952, A numerical method for solving the flow equation for water in unsaturated materials, *Soil Sci.* **73**, 105–116.
- Philip, J. R.: 1957, The theory of infiltration, 1. The infiltration equation and its solution, *Soil Sci.* **83**, 345–357.
- Protopapas, A. L. and Bras, R. L.: 1986, A model of plant growth and its relation to moisture and salinity transport in soil, Technical Report TR309, Ralph M. Parsons Lab., Mass. Inst. Of Technol., Cambridge.
- Protopapas, A. L. and Bras, R. L.: 1988, State-space dynamic hydrological modeling of soil-crop-climate interactions, *Water Resour. Res.* **24**(10), 1765–1779.

- Protopapas, A. L. and Bras, R. L.: 1990, Uncertainty propagation with numerical models for flow and transport in the unsaturated zone, *Water Resour. Res.* **26**(10), 2463–2474.
- Richards, L. A.: 1931, Capillary induction of liquids through porous mediums, *Physics* **1**, 318–333.
- Russo, D. and Bouton, M.: 1992, Statistical analysis of spatial variability in unsaturated flow parameters, *Water Resour. Res.* **28**(7), 1911–1925.